JMEPEG (2012) 21:988–994
DOI: 10.1007/s11665-011-9992-2

1059-9495/$19.00

Fatigue Behavior of Thin Sheets of DP590 Dual-Phase Steel

Sushil Kumar Giri and Debashish Bhattacharjee

(Submitted October 25, 2010; in revised form April 22, 2011)

Fatigue properties of 1.6 mm thick dual-phase steel (DP590) sheet have been determined by carrying out axial fatigue tests in load controlled mode at different stress ratios for both smooth specimens and specimens with hole at center. The presence of hole at center of the specimen significantly reduces the fatigue strength. When the fatigue data points are plotted in the Haig-Soderberg diagram, they follow a parabolic relationship for smooth specimens represented by Gerber line and a straight line relationship for the specimens with holes at its center represented by Goodman line. Master Diagram which acts as a guide for the fatigue design is also drawn for both smooth specimens and specimens with holes.

Keywords dual-phase steel, endurance limit, Goodman diagram, master diagram, stress ratio

1. Introduction

For automotive vehicles, there are conflicting requirements such as better fuel efficiency and better safety. In order to meet these requirements, steel being the most used automotive material should have higher strength to weight ratio. However, the properties such as ductility and formability of the steel decrease with increase in strength. In other words, the strongest steels which could make the largest savings in terms of weight can be the most difficult to form into different shapes. Hence, the ideal material for automobile applications will be the one which will have not only high strength, but also good ductility and good formability. These requirements led to a growing demand for steels like dual phase (DP) steel which in the form of thin sheets are used in the car bodies. As the automobile components experience varying load during service, this material requires to be evaluated in terms of fatigue properties. There have been various fatigue studies of this steel available in literature. Most of the studies concentrate on the influence of amount of martensite content on fatigue properties. Strain-controlled fatigue tests conducted by Wännman and Melander (Ref 1) show the increase of the cyclic stress with increase in martensite content. Sherman and Davies (Ref 2) found that cyclic stress is increased with increase in martensite content only up to 30% of martensite and beyond that the increase is marginal. Mediratta et al. (Ref 3) studied the influence of grain morphology of dual-phase steel on the fatigue properties. In their work, three kinds of microstructure have been studied namely (i) fine dispersion of martensite in fine-grained ferrite (Type I), (ii) continuous network of martensite around ferrite grains (Type II), and (iii) martensite islands encapsulated in a ferrite matrix (Type III). Type I microstructure showed the greatest resistance to fatigue failure when the material was tested in strain-controlled mode. Type III microstructure gave the most inferior fatigue life both in short- and long-life regime. Type II microstructure shows intermediate behavior. Sperle (Ref 4) have carried out experiments on different steels including different grades of dual-phase steels and then made a comparison of the results of these steels. Steels of similar strength show similar fatigue strength. Sudhakar and Dwarakadasa (Ref 5) have studied the influence of different amounts of martensite on the fatigue crack growth of this steel. Fatigue crack growth is decreased and threshold value of stress intensity range is increased with increase in martensite content.

Holes are present in most of the components for joining purposes (bolted or riveted joints) as well as for load bearing purposes. These holes severely decrease the life of the component by early fatigue failure and hence their effects on the fatigue properties are also required to be studied.

Although, there is a significant amount of work done on the evaluation of cyclic properties and fatigue crack growth rate of dual-phase steel, little work has been done to determine the effect of stress ratio on the fatigue properties of thin sheet of this steel. Also, in the literature, little data is available on the Goodman diagram and master curve for thin sheet of this steel. Hence, the purpose of the present investigation was to study the effect of stress ratio, stress concentrator like hole on resistance to fatigue failure, and then to draw diagrams such as Goodman diagram and master diagram. Master diagram can be used as a guide to design a component so that under a specified variation of stress, component does not fail in a required life period.

2. Experimental

DP590 steel with the chemical composition shown in Table 1 was employed in the present study. The tensile

Sushil Kumar Giri and **Debashish Bhattacharjee**, Research & Development Division, Tata Steel Ltd., Jamshedpur 831001, India. Contact e-mails: sushil.giri@tatasteel.com, sushilgiri_123@yahoo.com and dbhattac@tatasteel.com.

properties of this steel have been tabulated in Table 2. The steel has a two phase microstructure, namely martensite (white phase) and ferrite (other phase) as shown in Fig. 1. Fatigue specimens with configurations shown in Fig. 2 were machined out of 1.6-mm thick sheets keeping the longitudinal direction of the specimens along the rolling direction of the sheet.

The specimens were then polished using different grades of emery papers with final polishing done with the 1000 grade polishing paper. Roughness details measured on one of the polished surface of the specimen are as follows. R_a = 0.1 μm, R_z = 0.67 μm, R_y = 1.04 μm, peaks per mm is 8.8/mm, where, R_a is average roughness, R_z is average maximum height of the roughness profile, R_y is maximum height of the profile. In order to study, the effect of stress concentrator on fatigue properties of this steel, some specimens with a hole at the center of the reduced section are used in the experiment. These holes were made by drilling and then the surface of the hole bores were polished with a diamond file in order to remove the burrs or coarse machining marks. The diameter of the hole is approximately 2 mm. Axial fatigue experiments were carried out using a 25 kN INSTRON servo hydraulic machine in load-controlled mode at stress ratios, $R = -1, -0.67, -0.33, 0.1, 0.33$ as per ASTM E466 standard.

A sinusoidal waveform was selected for these experiments and the frequency of loading was kept at 20 Hz. For negative stress ratios, i.e., $R = -1, -0.67, -0.33$, an antibuckling unit was mounted onto the specimens in order to prevent buckling of the specimens. At each stress ratio, the tests were conducted at different values of maximum stresses and then the corresponding number of cycles to failure was noted. The tests were run until the specimen failure occurred and for nonfailure cases, the test was terminated at 5 million cycles. After the fatigue tests, the fractography samples were cut from the broken specimens and then the fracture surfaces were observed under scanning electron microscope.

Table 1 Composition of DP590 steel (wt.%)

C	Mn	Si	S	P	Ti
0.09	0.98	0.31	0.005	0.013	0.002

Table 2 Tensile test properties of DP590 steels

YS, MPa	UTS, MPa	% Elongation
390.5	614	26.55

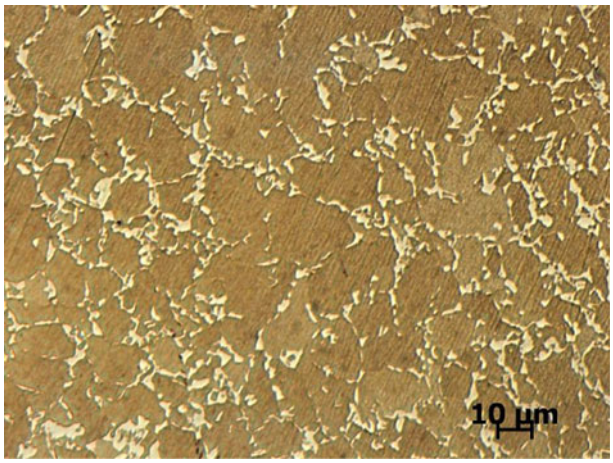

Fig. 1 Microstructure of dual-phase steel (DP590) (white phase: martensite, ferrite: other phase)

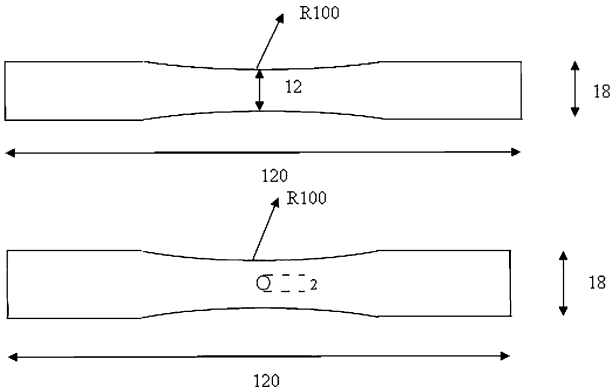

Fig. 2 Configuration of the specimens. All dimensions are in mm

3. Results and Discussion

3.1 Effect of Stress Concentration

The S-N curve for smooth specimen of this steel is shown in Fig. 3 for a stress ratio of −1. The open marker in the figure corresponds to the specimens which did not fail in 5 million cycles. The same curve is plotted in Fig. 4 but the *X*-axis is not in logarithmic scale. The data are fitted with a line representing the power curve relationship. The equation of this line is of the form of Basquin's equation, $\sigma_a = \sigma_f N_f^{-b}$, where σ_a is the stress amplitude, N_f is the number of cycles to failure, σ_f is the fatigue strength coefficient, and b is the fatigue strength exponent. The values of these constants are shown in Table 3 for a stress ratio of −1.

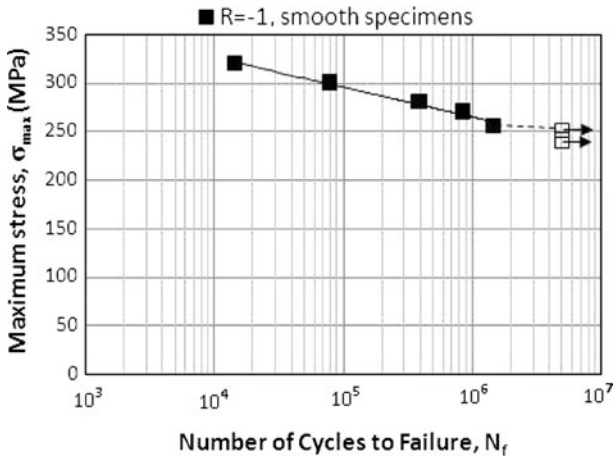

Fig. 3 S-N Curve for DP590 steel at $R = -1$. Open markers represent specimens which have not failed till 5 million cycles

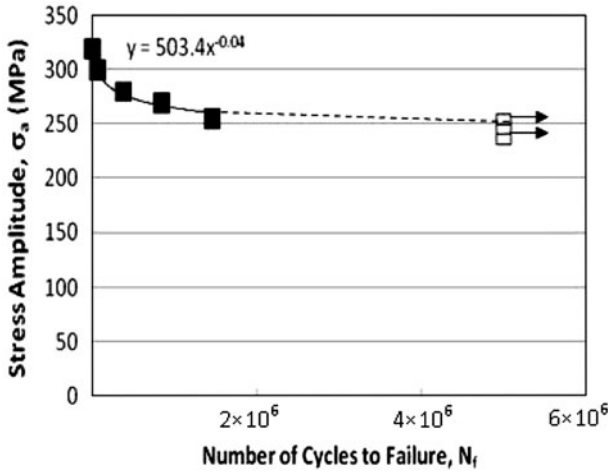

Fig. 4 S-N Curve for DP590 steel at $R = -1$ represented by Basquin's equation. Open markers represent specimens which have not failed till 5 million cycles

Table 3 Basquin's constants

Type of specimen	σ_f	b
Smooth	503.4	0.04
Hole	831.7	0.11

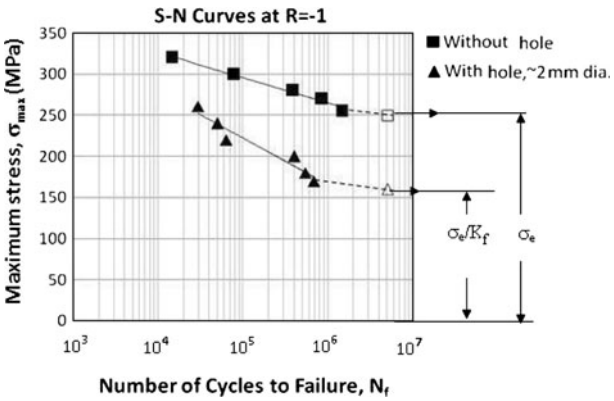

Fig. 5 Fatigue life is decreased in specimens having hole at center when compared with smooth specimens. Open marker represents stress levels at which the specimen has sustained

Figure 5 shows the effect of a hole drilled at the center of the specimen on the S-N curves for a stress ratio of −1. For the specimens with hole, the stress is calculated using the net cross section of the specimen. Net cross section is calculated by multiplying thickness with a value which is equal to width at the center of the specimen minus the diameter of the hole. The presence of hole is found to decrease the endurance limit from 250 to 160 MPa. It is also observed that the difference between the stress levels for a specified number of cycles to failure is higher toward the high cycle regime. This may be due to the higher notch sensitivity at lower stress and high cycle region. At high stress and low cycle region, the plastic deformation may be significant which may have alleviated the effect of stress concentration and thus notch sensitivity.

The endurance limits, defined for 5 million cycles without failure, are shown together with the fatigue strength reduction factor and the fatigue ratio in Fig. 6(a) and (b). Fatigue strength reduction factor (K_f) is defined as the ratio of the fatigue strength of smooth specimen and that of specimen with hole. Hence, K_f for a stress ratio of −1 = 250/160 = 1.56. Fatigue ratio defined as the ratio between the endurance limit and the UTS of the material are found to be 0.407 and 0.26 for smooth specimens and specimens with a hole, respectively. The notch sensitivity factor of the material, q, defined as $(K_f - 1)/(K_t - 1)$, is equal to 0.358 for a stress ratio of −1. Here, K_t is the stress concentration factor which is expressed by the following equation (Ref 6).

$$K_t = 2 + (1 - d/w)^3,$$

where d is the diameter of the hole and w is the width of the specimen at its center. Hence, stress concentration factor, K_t for the specimen having 12 mm width and a 2 mm diameter hole at center of the specimen = 2.57

3.2 Effect of Stress Ratio

Figures 7 and 8 show the effects of stress ratio on the S-N curves. With increase in stress ratio, the curves shift upward. In other words, when the specimens are tested at two different stress ratios for a given maximum stress, the specimen tested at higher stress ratio will take more cycles to fail than the other one. This may be because of the following reasons. The fatigue failure occurs mainly in two stages: (i) crack initiation and (ii) crack propagation. However, in high cycle fatigue, crack initiation is involved during the major portion of the total cycles to failure, compared to crack propagation. Hence, the fatigue life for this high cycle fatigue is dependent mainly on the crack initiation which occurs by slip band formation. Both compressive as well as tensile stresses contribute to the fatigue damage in the form of this slip band formation. Hence, the total number of cycles to failure depends not only on the maximum stress, but also on the range of stress. For a constant maximum stress, the range of stress at $R = -1$ is more than that at $R = 0.1$. More is the range of stress, more is the fatigue damage in the material. Hence, the number of cycles to failure at $R = -1$ is less than that at $R = 0.1$. It is also to be noted that the endurance limit is found to be increasing with increase in the value of stress ratio.

The fatigue data corresponding to nonfailure of specimens till 5 million cycles can be represented in form of a diagram called Goodman diagram as shown in Fig. 9. This diagram is drawn taking maximum stress and minimum stress along the *Y*-axis and mean stress along the *X*-axis. The curves of dash type in the figure correspond to specimens having holes at center, whereas the solid curves are for smooth specimens. It is evident from this diagram that the slope of the curve for the maximum stress corresponding to specimens with hole is lower than that of the smooth specimens. Also, from Fig. 6(a), it can be seen that with increase in R, the rate of increase of endurance limit for specimens with hole is less compared to smooth specimens. It may be because of the fact that the effect of stress concentration is more dominant than the effect of increase in R. The stress concentrator like hole raises the local stress around the hole to a value much higher than the nominal stress. This helps in early crack initiation thereby causing early fatigue failure. Hence, the endurance limit for specimens with holes does not increase at a rate at which it occurs for smooth

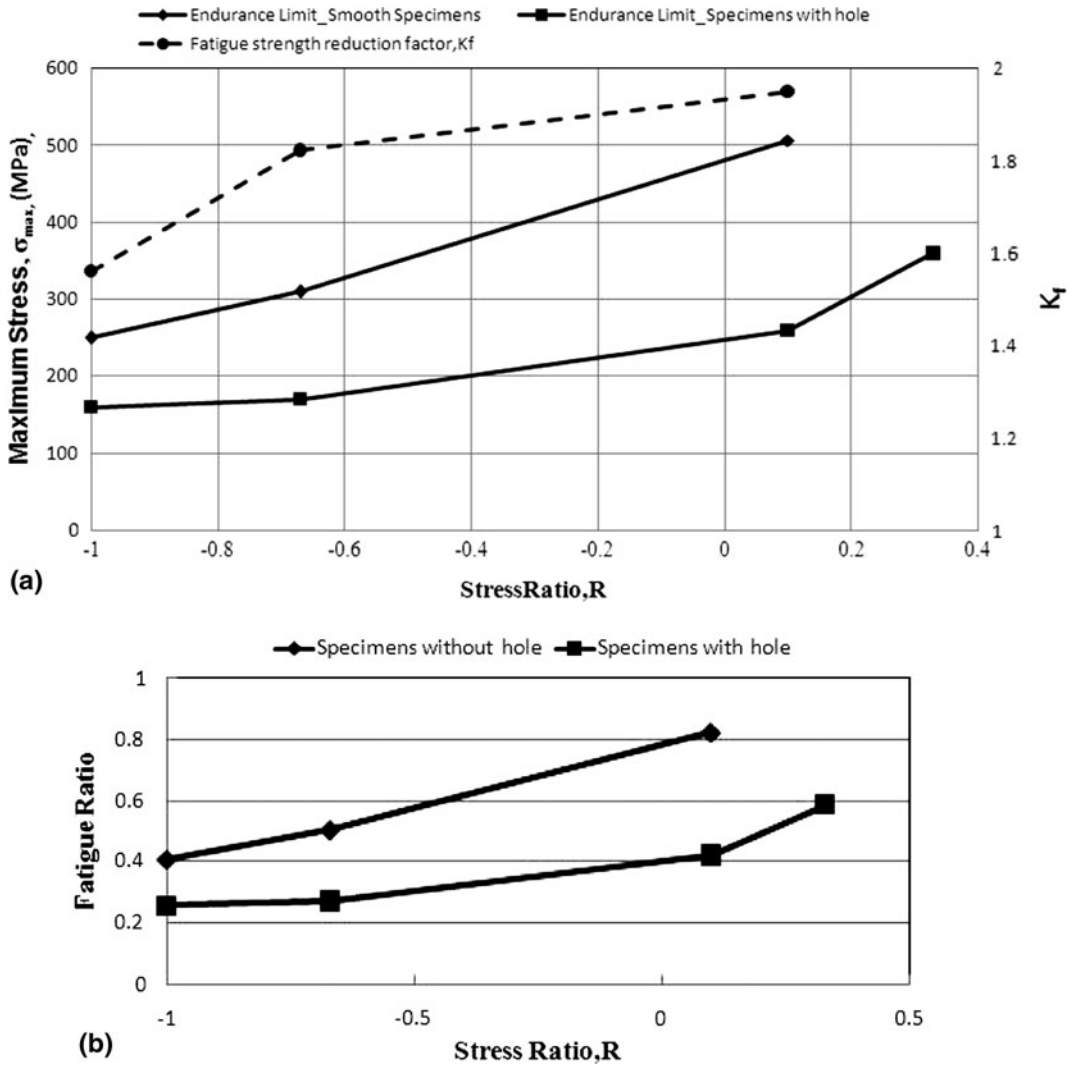

Fig. 6 (a) Variation of endurance limit and fatigue strength reduction factor with stress ratio. (b) Variation of fatigue ratio with stress ratio

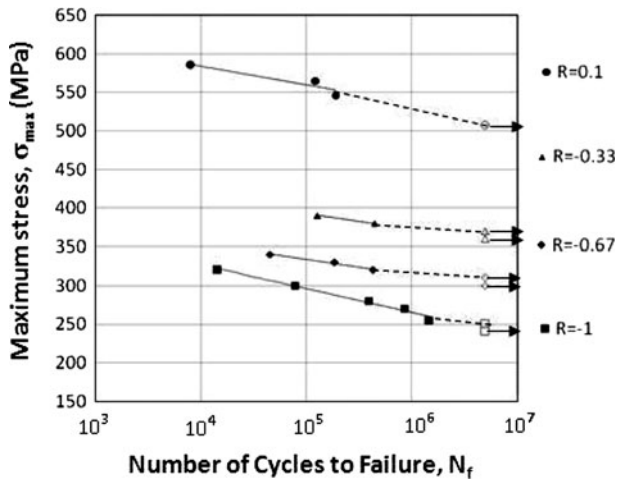

Fig. 7 S-N curves for smooth specimens

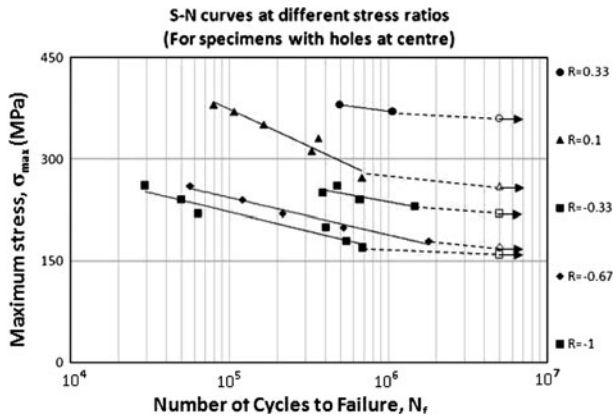

Fig. 8 S-N curves for specimens with holes at the center

specimens. It is also observed that at stress ratio of 0.1, the smooth specimen does not fail at stresses below yield strength, i.e., 390 MPa.

Usually fatigue data are determined for conditions of reversed cycles of stress, i.e., mean stress, $\sigma_m = 0$. In order to find the effect of other types of loading, a diagram called Haig-Soderberg diagram is drawn between stress amplitude and the mean stress as shown Fig. 10. This diagram shows the combination of alternating stress and mean stress at which the

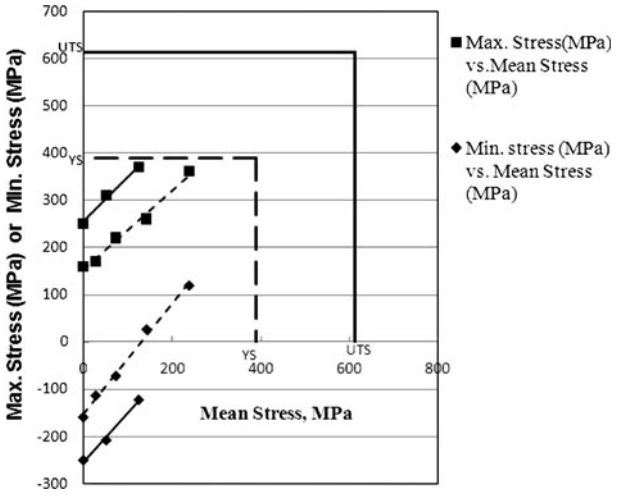

Fig. 9 Goodman diagram for smooth specimens

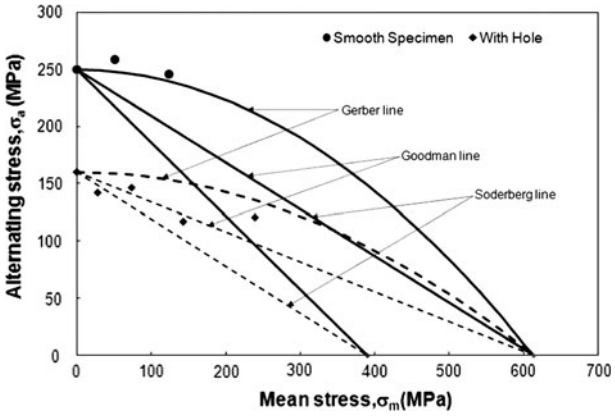

Fig. 10 Haig-Soderberg diagram

material will sustain 5 million cycles (which corresponds to the endurance limit). The straight line drawn from the endurance limit to the ultimate tensile strength is called the Goodman line. Therefore, for a given situation of fatigue loading, if the data point lies toward the left side of this line, then it is assumed that the component will sustain 5 million cycles. Otherwise, it will fail before these many cycles. Gerber proposed a parabolic relation, while Soderberg proposed a more conservative relationship, i.e., the straightline from endurance limit for $R = -1$ to yield strength of the steel. After carrying out the tests at different stress ratios, the endurance limits in terms of stress amplitude and mean stress are superimposed on this diagram. Much of the data related to endurance limit of different materials are available in literature. According to Forest (Ref 7), 90% of fatigue data (endurance limit) for ductile metals lie above the Goodman line and two-third of the data lie between the Goodman line and Gerber line. The fatigue data for 4130 steel lie very close to the Gerber line as per Grover et al. (Ref 8). Similarly, for nonferrous metal Gerber line is a bit conservative as the data are lying above the Gerber line (Ref 9). However, for the dual-phase steel used in our experiments, it is found that, the test data for smooth specimens are falling close

Table 4 Equations for S-N curves

Smooth specimens		Specimens with hole at center	
R	Equation of S-N curve	*R*	Equation of S-N curve
−1	$\sigma_{max} = -15.2\ln(N_f) + 473.4$	−1	$\sigma_{max} = -24.5\ln(N_f) + 504.8$
−0.67	$\sigma_{max} = -8.71\ln(N_f) + 434$	−0.67	$\sigma_{max} = -23.3\ln(N_f) + 511.7$
−0.33	$\sigma_{max} = -7.98\ln(N_f) + 483.8$	−0.33	$\sigma_{max} = -18.9\ln(N_f) + 498.6$
		0.1	$\sigma_{max} = -47.1\ln(N_f) + 916.5$
		0.33	$\sigma_{max} = -13.1\ln(N_f) + 551.8$

to Gerber line, whereas for specimens with holes, they are falling close to Goodman line as shown in Fig. 10. Therefore, for dual-phase steel, it appears that Gerber equation would be a good approximation for parts without stress concentrator and for parts with stress concentrator like hole, Goodman equation is more appropriate.

3.3 Construction of Master Diagram

The experimental data for each stress ratio shown in Fig. 8 and 9 are curve fitted separately with equations of the logarithmic form like $y = a\ \log(x) + b$, where a and b are constants. Therefore, for each stress ratio, the corresponding equations are obtained and then they are used to find out the maximum stresses for different cycles to failure such as 10^4, 10^5, and 10^6 cycles. The equations used are tabulated in the Table 4 as follows. Then, the master diagram as shown in Fig. 11 is drawn. Each line in this diagram is drawn by connecting the data points corresponding to a cycle to failure. At the bottom of the diagram, identification of the data points is given. The curves represented by solid line are for smooth specimens. This diagram is very useful from the point of view of design against fatigue. It is possible to select the combination of mean stress and stress amplitude that can be applied on a component for sustaining a certain number of cycles to failure. For example, if a component is required to sustain $>10^4$ cycles but $<10^5$ cycles, then the stress amplitude and the mean stress should be such that the corresponding data point should lie between the constant cycle lines represented for 10^4 cycles and 10^5 cycles in the master diagram. Similar diagram is drawn for specimens with hole and it is superimposed on the diagram for smooth specimens. However, this diagram is exclusively for a component with a stress concentration factor, $K_t = 2.57$.

3.4 Fractography

The fractographic examination of fracture surface of smooth specimens shows that the crack is starting from the surface as shown in Fig. 12(a) and (b). Figure 13(a) and (b) shows the crack initiation sites for specimens with hole. The cracks are initiating from locations near the surface of the hole bore and they are propagating in the width direction toward the outside edge of the specimens which is seen from Fig. 14. In comparison to the fractograph for smooth specimens, crack initiations seem to have occurred from more than one site in specimens with hole. Figure 15(b) shows typical striation marks which are characteristics of fatigue crack propagation on

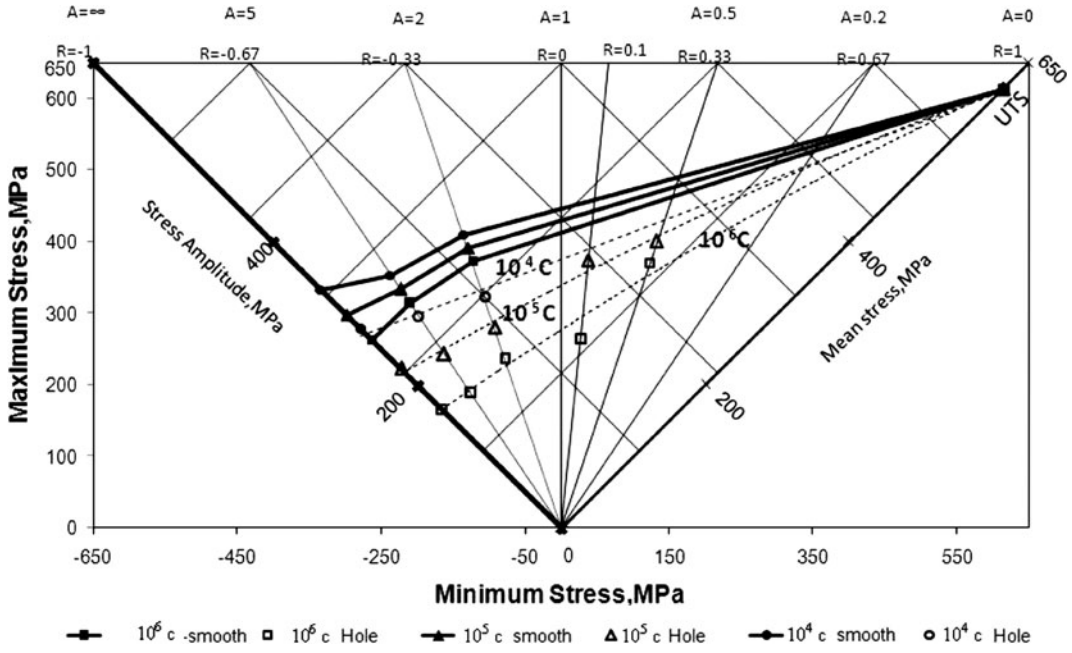

Fig. 11 Master curve for DP590 steels

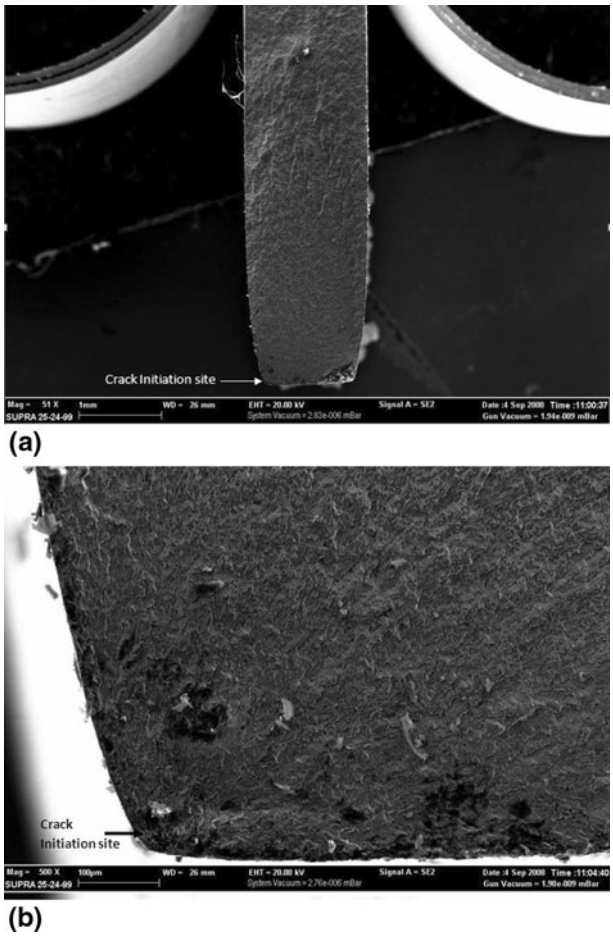

Fig. 12 (a) Crack initiation site in fracture surface of smooth specimens. (b) Crack initiation site in fracture surface of smooth specimen at 500×

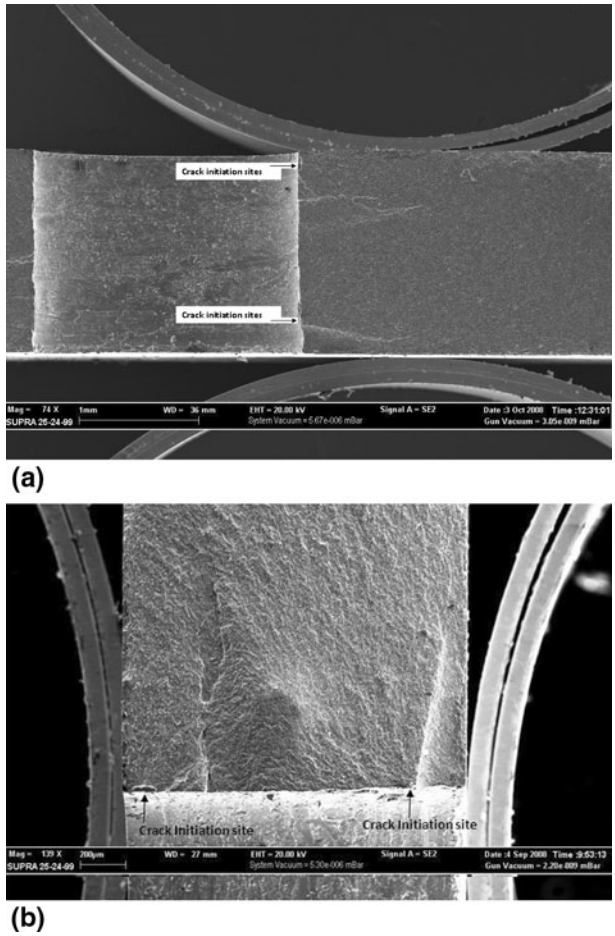

Fig. 13 (a) Crack initiation site in fracture surface of specimen with hole. (b) Crack initiation sites in fracture surface of specimen with hole at 139×

Fig. 14 A portion of the specimen showing the path of crack propagation

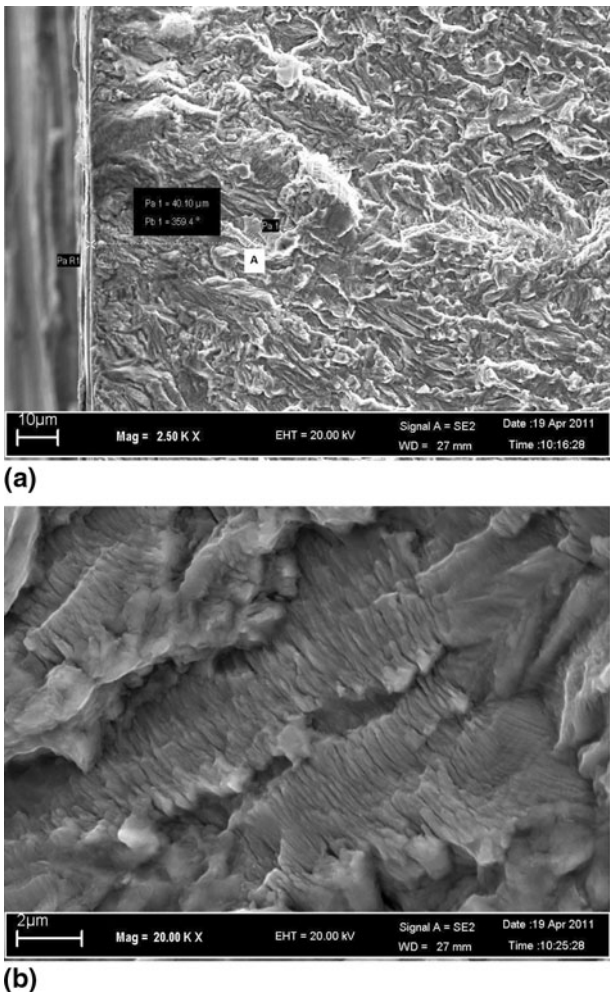

Fig. 15 (a) Fractograph in one of the specimen with hole. The point A is the location at which the fractograph in Fig. 14(b) is taken. (b) Striations on fracture surface of specimen with hole at the location A mentioned in Fig. 14(a)

the fracture surface of the specimens with hole and the location at which this fractograph is taken is 40.1 µm away from the crack initiation site as shown in Fig. 15(a).

4. Conclusion

1. Increase in R, increases the endurance limit of the material.
2. Stress concentration as a result of a hole at the center of the specimen significantly reduces the fatigue strength. For instance, the decrease in fatigue strength due to the presence of the hole of diameter ~2 mm is by a factor of 1.56 at stress ratio (R) of −1.
3. The effect of stress concentrator is more dominant than the effect of increase in stress ratio (R). This is evident from the fact that with increase in R, the fatigue strength reduction factor is found to increase. In other words with increase in R, the increase in endurance limit for specimens with hole is not as significant as that for smooth specimens.
4. For dual-phase steel, Gerber equation would be a good approximation for calculating the endurance limit for parts without stress concentrator and for parts with stress concentrator like hole, Goodman line is more appropriate.
5. Master diagram has been developed for 1.6 mm DP590 steel sheet. This will be useful to select the range of stress for which the component will be designed to sustain a specified number of cycles.

Acknowledgments

The authors are grateful to Prof R. K. Ray, visiting scientist, R&D, Tata Steel Ltd. and Ms. Shrabani Mazumdar, Researcher, R&D, Tata Steel Ltd. for their valuable comments and suggestions.

References

1. L. Wännman and A. Melander, Influence of Martensite Contents and Properties on Fatigue Behaviour of Dual-Phase Sheet Steels, *Mater. Des.*, 1991, **12**(3), p 129–132
2. A.M. Sherman and R.G. Davies, The Effect of Martensite Content on the Fatigue of a Dual-Phase Steel, *Int. J. Fatigue*, 1981, **3**(1), p 36–40
3. S.R. Mediratta, V. Ramaswamy, and P. Rama Rao, Influence of Ferrite-Martensite Microstructural Morphology on the Low Cycle Fatigue of a Dual-Phase Steel, *Int. J. Fatigue*, 1985, **7**(2), p 107–115
4. J.O. Sperle, Fatigue Strength of High Strength Dual-Phase Steel Sheet, *Int. J. Fatigue*, 1985, **7**(2), p 79–86
5. K.V. Sudhakar and E.S. Dwarakadasa, A Study on Fatigue Crack Growth in Dual Phase Martensitic Steel in Air Environment, *Bull. Mater. Sci.*, 2000, **23**(3), p 193–199
6. W.D. Pilkey and D.F. Pilkey, *Petersons Stress Concentration Factors*, Chapter 4, 3rd ed., John Wiley and Sons, 2008, p 183, eq. 4.9
7. P.G. Forrest, *Fatigue of Metals*, Pergamon Press Inc., London, 1962
8. H.J. Grover, S.M. Bishop, and L.R. Jackson, "Axial Load Fatigue Tests of Unnotched Sheet Specimens of 24S-T3 and 75S-T6 Aluminium Alloys and SAE 4130 Steels," Technical Note 2324, National Advisory Committee for Aeronautics, 1951
9. F.M. Howell and B.J. Lazan, Axial Stress Fatigue Strength of Several Structural Aluminum Alloys, *Proc. Am. Soc. Testing Mater.*, 1955, **55**, p 1023–1026